

Damage Assessment of Long-span Bridges using GPS/Accelerometer Observations under Dynamic Effects

Mosbeh R.KALoop, Korea; Mohamed A.SAYED, Canada; Jong-Wan HU, Korea

Keywords: RTK-GPS; Accelerometer; Bridge; Time and Frequency Domain

SUMMARY

This study investigates at evaluating long span bridges using the integrated real-time kinematic global positioning system (RTK-GPS) and accelerometer technique. The data were collected from structural health monitoring system that installed on Yonghe cable-stayed bridge, China. A high-rate (20 Hz) GPS and 100 Hz accelerometer were utilized and integrated to observe the bridge behavior. A healthy and damage cases are evaluated under complicated loads, including traffic and ambient environmental loads effects. The time and frequency domains and numerical model were applied to assess the integrated system. The analysis of the results of the integrated system showed high correlation between the GPS/accelerometer observations in both time and frequency domains, particularly after occurrence of the damage. In addition, the GPS/accelerometer system observations demonstrate the significant efficiency of GPS observations for the damage in the time domain, while the accelerometer observations seem more effective in investigating effect of the damage in the frequency domain.

Damage Assessment of Long-span Bridges using GPS/Accelerometer Observations under Dynamic Effects

Mosbeh R.KALOOP, Korea; Mohamed A.SAYED, Canada; Jong-Wan HU, Korea

1. INTRODUCTION:

Vibration and high dynamic effects acting on long span bridges are critical for their lifetime. Therefore, there are many sensors, such as Global Positioning System (GPS), displacement, strain, accelerometer sensors are used to measure the performance of bridges (Zinno et al. 2019; Im et al. 2013; Chang et al. 2003). Dynamic observation, analysis, identification, and damage detection are considered among the main aims of developed structural health monitoring (SHM) systems. Thus, this study investigates whether possible of bridges time and frequency properties can be detected using integration GPS/Accelerometer measurements.

The main behaviors of long span bridges are the deflection and vibration of deck and towers of it (Zhang et al. 2013). The GPS is considered one of the important sensors used to measure structures' static and quasi-static displacements (Kaloop et al. 2017). The advantages and disadvantages of GPS to monitor structures' movements are summarized in Yi et al. (2013). Nevertheless, the measurements noises and errors affect the GPS measurements accuracy as presented and discussed in Roberts et al. (2004). The GPS measurements of structures' movements are always contaminated by noise, multipath and GPS errors effects (Yi et al. 2012; Moschas and Stiros 2013; Kaloop and Hu 2015). Therefore, measurements' filtration and smoothing should be applied before analyzing them. Furthermore, preliminary studies have proven the ability to use real time kinematic (RTK)-GPS to monitor dynamic deformation of structures due to winds, traffic, earthquakes, and similar loading cases and to eliminate effects of GPS errors (Roberts et al. 2004; Im et al. 2013). Accelerometers are, also, among the sensors used to measure structures' dynamic displacement (Hwang et al. 2012). As such, monitoring structures using accelerometers enables extracting structures' acceleration response up to 1000 Hz natural frequency because of its high sampling frequency (Chan et al. 2006).

Recently, efforts have been made to use an integrated monitoring system consists of RTK-GPS dual frequency receivers and accelerometers for structures dynamic evaluation (Roberts et al. 2004; Hwang et al. 2012). The integration of accelerometers with the RTK-GPS significantly increases the measurement production and improves the overall reliability and performance of the system (Li et al. 2006; Meng et al. 2007). In this study, the GPS/accelerometer integrated system is analyzed. A novel analysis to assess the full performance of structures based on extracted quasi-static and dynamic movements in time and frequency domains of the integrated system is presented. The basic challenge is that damage is typically a local phenomenon and may not affect the global frequency response of a structure normally measured during vibration tests. Environmental and operational variations, such as moisture, varying temperature, and loading conditions affecting structures' dynamic response cannot be overlooked. Moschas and Stiros (2013) stated that the frequency range 0.4~5.0 Hz covers a wide variety of dynamic motions, including oscillations of most engineering structures and earthquake events. In addition, frequency range 0~0.4Hz corresponds to quasi-static displacement, for instance slow displacements induced by temperature changes, and the

corresponding long-period displacements component are to a smaller or larger degree contaminated by colored noise (Moschas and Stiros 2013). Doebling *et al.* (1996) summarized previous studies and methods used for structures' damage detection, the statistical analyses and fundamental frequency changes were used to detect the structures behavior in time and frequency domains, respectively. Moreover, frequency changes exceeding 10 % occur when a structural modification was implemented that resembled a structural failure (Doebling *et al.* 1996). However, in this study, the assessment of the damage effects is presented to understanding the behavior of a long span bridge under damage case; and the evaluation of the proposed methods for damage detection is discussed.

2. OBSERVATIONS AND METHODS

2.1. Bridge description and SHM system

The Yonghe Bridge is a cable-stayed bridge connecting Tianjin and Hangu cities in China, Figure 1. It consists of a main span of approximately 260 m and two side spans of 125 m each, carrying two traffic lanes with total width of 14.50 m. The two door-shaped towers are reinforced concrete members with total height of 60.50 m. After 19 years of operation, repairs were performed between the years 2005 and 2007. For that, a monitoring system was designed. Different sensors are used in the SHM system of the bridge, Figure 1. Among these sensors, fourteen uni-axial and one bi-axial accelerometers were permanently installed on the different location of the bridge deck; while one accelerometer was insulated on tower summit point (100 Hz). Moreover, to measure the wind velocity and ambient temperature, an anemoscope and temperature sensors were attached to the bridge tower and deck, respectively. Two GPS units were permanently installed on the two towers, while a third one was located on the river bank near the bridge as a base point based on RTK observation technique. 20 Hz receivers (LEICA GMX902 antenna) were used to monitor the bridge. Using GPS Spider 2.1 software, the data was pre-processed in the WGS84 coordinate system. Kaloop and Hu (2016) have assessed the GPS measurements and they concluded that the GPS positioning accuracy is better than ± 6 mm; with acceptable accuracy of the GPS measurements. Hence, the time sequences of each station positions located on the bridge were generated.

The data of the GPS and accelerometer were recorded simultaneously, and they installed at the same level position of the bridge tower. The two different measurements sets are considered in this study as a system of integration monitoring system. For the analysis and evaluation of the observed data, local bridge coordinate system was established (Roberts *et al.*, 2004). The data analysis was based on the data collected and converted to the bridge local coordinate system (BCS) in the X-(which shows the lateral direction for the local BCS) and Y-(which shows the longitudinal direction for the local BCS) directions. The X and Y movements are greater than that reported in the Z-direction, thus the Z-direction movements were declined.

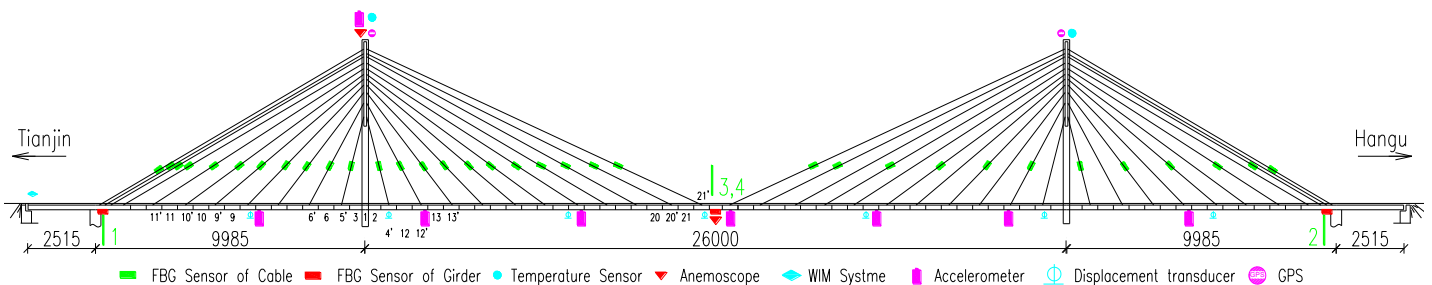


Figure 1. Bridge elevation and monitoring system

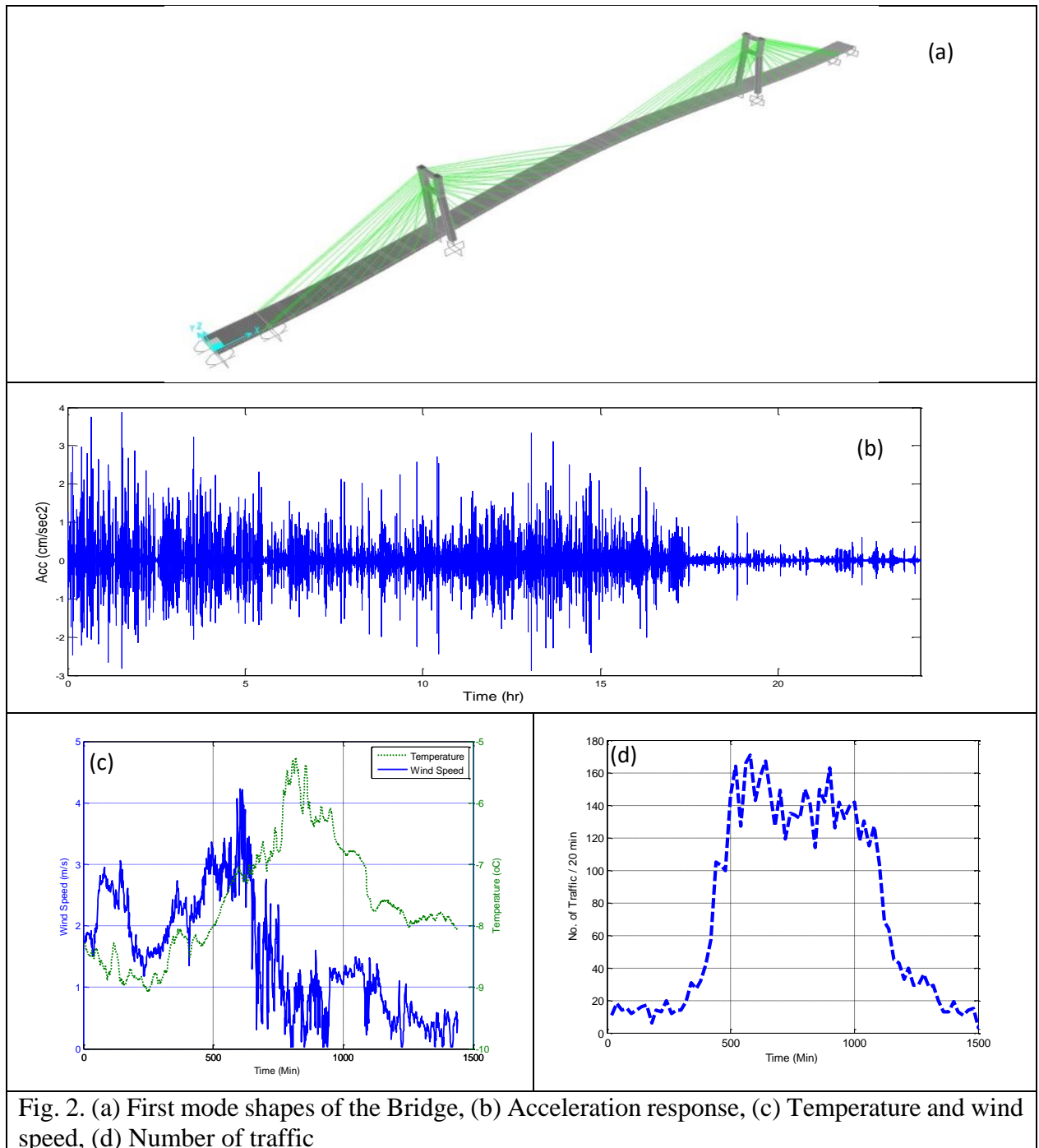
2.2. Numerical model of Yonghe Bridge

A three-dimensional FEM of the Bridge was established and implemented using the SAP2000 software to analyze the movements of the bridge tower. The bridge towers and the main girder were modeled using the beam elements. Transverse concrete beams were modeled as additional mass elements. Eighty-eight cable elements were used to model all the cables with variable cross-sectional area from 78.14 cm^2 to 27.10 cm^2 . In addition to that, ambient environmental loads (wind and temperature) and moving vehicle loads as shown in Fig. 2.c&d were considered in the proposed model. Also, uniform dead load of 1.90 t/m was used to consider all the main girder secondary loads. The main girder was modeled as floating on the bridge towers, while both towers are fixed to the ground. Moreover, the longitudinal restriction effect of the rubber support is simulated using linear elastic spring elements. The bridge was modeled considering the varying temperature and wind speed. Figure 2.a shows the modal frequencies and the first mode shape. The bridge first five modal frequencies are 0.3033 Hz , 0.4063 Hz , 0.6158 Hz , 0.7966 Hz and 0.8151 Hz , respectively. The calculated frequencies are used to guide the corner frequencies for the filter design in the next sections.

2.3. Procedure of Data analysis

This study is investigating the southern tower behavior, located in the side of the Tianjin city. The analysis of the southern tower' movements in both X- and Y-direction are presented. The observations of the integrated GPS/accelerometer system are studied and analyzed in two situations: (1) before the damage occurred, which observed on January 17th, 2008; and (2) after the bridge damage, which measured on July 31st, 2008.

The observations of the integrated GPS/accelerometer in both time and frequency domains are investigated. Figs.2.c and d illustrate the average temperature and wind speed changes and number of vehicles during one January 17, 2008. The traffic monitoring point is fixed at the entrance of the bridge at Tianjin direction. From Figure 2, the maximum wind speed is about 4 m/sec with average temperature difference of $3.8 \text{ }^\circ\text{C}$, and the maximum number of passed vehicles 171. Kaloop and Li (2014) studied the tower movements under the load effects and they found that the traffic loads are the main cause of the tower movements. Furthermore, the dramatically amplitude drop of acceleration (Fig.2.b) is occurred after traffic elimination and it is concluded that the traffic load is dominant.



2.3.1. Data Filtering of GPS Observations

As per the previous studies, e.g. (Moschas and Stiros 2013) the GPS observations are contaminated by noises. Therefore, filters should be applied to de-noise the time series displacement components (Moschas and Stiros 2011). The GPS software produces the Cartesian coordinates time series of the rover receiver in the WGS'84 coordinate system. The horizontal BCS (d_i), which we examined in the present paper, were transformed into a time

series of apparent displacements h_i in the X- and Y-direction around a relative zero representing the equilibrium level of the monitored point. This similarity transformation was based on Eq.1:

$$h_i = d_i - 1/n \sum d_i \quad (1)$$

Where, $i=1,2,3,\dots,n$, n are the total number of observations interval, while d the observations values represents in the X- and Y-direction.

In this study, the low-pass Moving Average (MA) filter is used to de-noise the apparent GPS observations and to extract the relative quasi-static (smoothed) displacements components of the bridge tower. Moreover, the high-pass MA filter (a moving average filter with a step of approximately 2 min.) combined with the band-pass filter are used to extract the dynamic displacement component of the tower in the two monitoring cases from short-period component that is the supervised learning-derived filtering, i.e. before and after the occurrence of damage. The low pass and high filter design based the first mode SAP model pronounced at 0.3033 Hz. Figures 3 (a)&(b) illustrate the extracted tower displacement components from GPS observations in X-direction before and after data filtering.

2.3.2. Frequency Identification of GPS/Accelerometer

Fast Fourier Transform (FFT) is used to transform the observations of the GPS and accelerometer from time to frequency domain (Li *et al.*, 2006). Also, the frequencies components power spectrums are calculated. The frequency domain analysis is conducted for the fundamental frequencies of the GPS and accelerometer acceleration measurements. The GPS displacement observations in the X- and Y-direction are converted to acceleration time series using the double differentiation procedure. In addition, low and high pass filters are applied to extract the semi-static and dynamic displacement components of the tower based on the extracted fundamental (first mode) frequency from the FEM model of the bridge.

3. RESULTS AND DISCUSSION

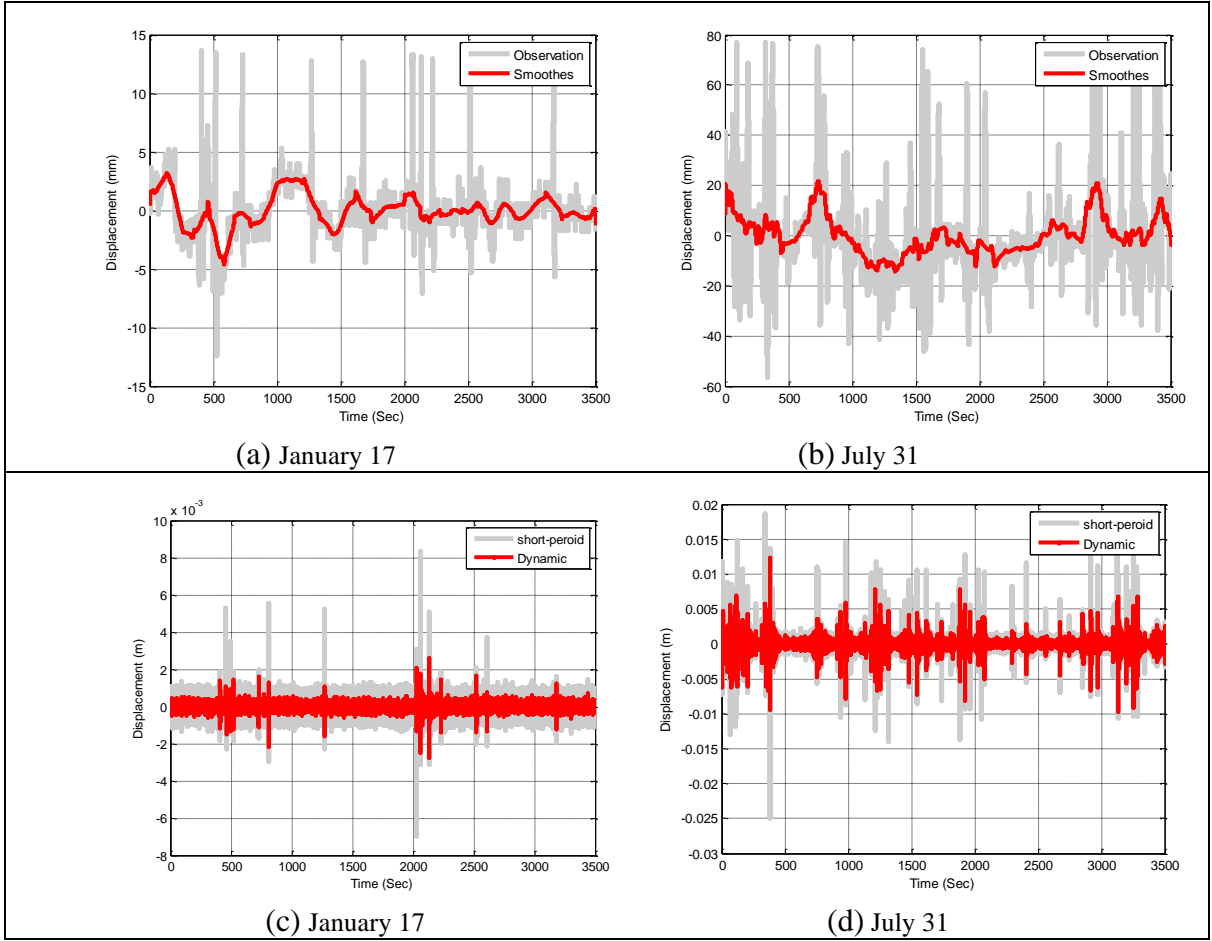
3.1. GPS Displacement Components

The bridge tower displacement components from the GPS observations are discussed. The original and smoothed GPS relative displacement observations after applying the MA filter during one-hour observation before and after the occurrence of the damage (Figs. 3-a and 3.b, respectively). The filters are applied with a corner frequency that extracted by FEM. The correlation coefficient (R) between the original and smoothed displacement observations is 0.82 and 0.65 before and after damage, respectively. This indicates that the frequency contents of the filter signals are almost comprises the signal frequencies without information losses. Therefore, MA filter can be used to extract the quasi-static displacement components.

Figures 3-c and 3-d illustrates the GPS dynamic and short period displacement component, which comprises the dynamic components of the measurements and dynamic noises, during one-hour observation before and after the damage occurrence, respectively. The short period displacement is extracted from the smoothed displacement observations after applying the high pass filter. After that, the dynamic period displacement is extracted after applying the band pass filter to remove the dynamic noises. In addition, the high GPS displacement amplitude of both original and smoothed observations is shown clearly due to the damage and cracks occurrence in the bridge. Moreover, high correlation (0.85) between short period and dynamic displacement components with no displacement information losses in both

dates. Consequently, the short period and dynamic components can be used to extract the frequency domain components in the case of damage. Therefore, applying the MA combined with the band pass filter is recommended to extract the dynamic displacement components from GPS observations and these results are concluded in (Moschas and Stiros, 2011, 2013).

Furthermore, Figs. 3-(e) and (f) demonstrate the statistical quasi-static GPS displacement component of one day observations before and after damage occurrence. The results illustrate that the maximum quasi-static displacements are 16.0 mm and 9.8 mm in the X- and Y- directions, respectively, before the damage occurrence. In addition, the maximum quasi-static displacements are 30.5 mm and 23.3 mm in the X- and Y-directions, respectively, after the damage condition. Furthermore, the displacement range is between 40.78 mm and 32.51 mm before damage, while it is between 60.73 mm and 43.52 mm after damage in X- and Y- directions, respectively. The standard deviation calculation is shown approximately equal. Thus, the statistical maximum and minimum with mean quasi-static displacement can be utilized to detect the damage effect. Herein, from Figs. 2.b and 3.e-f, the damage has occurred during July, as the defamations show high values.



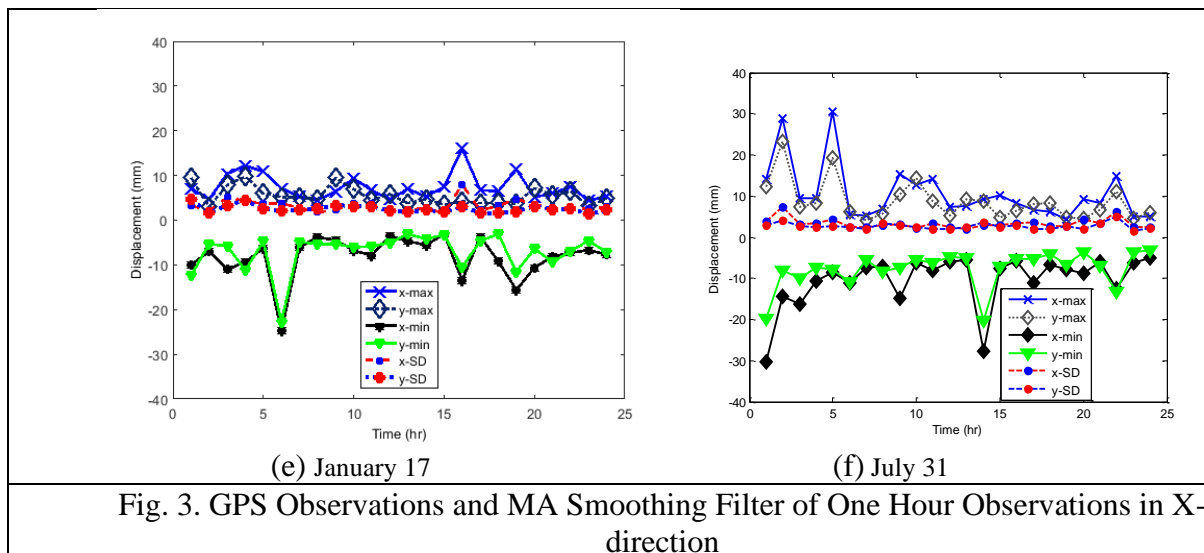


Fig. 3. GPS Observations and MA Smoothing Filter of One Hour Observations in X-direction

3.2. Comparative Dynamic Displacements of GPS and Accelerometer Measurements

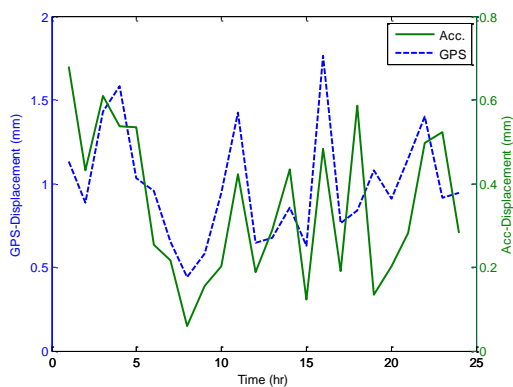
Figure 4 shows the maximum dynamic displacement component of the tower 24-hours observations in both X- and Y-directions before and after the damage, respectively. The GPS dynamic component is calculated as illustrated in the previous section, while the accelerometer dynamic component is derived from the double integration of the recorded acceleration time histories with the band pass filter (Hwang *et al.*, 2012). The band pass filter is applied with a corner frequency (0.3033 Hz) that represents the bridge fundamental frequency calculated from the FEM.

The quantitative comparison of both the GPS observations dynamic displacement and the accelerometer observations integrated dynamic displacement may not be realistic, since the static and quasi-static displacement components are missing from the accelerometer-derived displacement results (Li *et al.*, 2006). Figure 4-(a) illustrates good correlation (0.63) between the GPS and accelerometer observations maximum dynamic displacement in the X-direction, which represents the bridge tower cables direction, in the undamaged monitoring case on January 17th. This result indicates that the tower vibrations totally depend on the cables forces and vibrations. In addition, Fig. 4-(b) shows less correlation (0.41) due to the lack of dynamic vibrations in the Y-direction. This direction is only affected by wind forces and the relative vehicle case of loading on the two-lanes of the main girder.

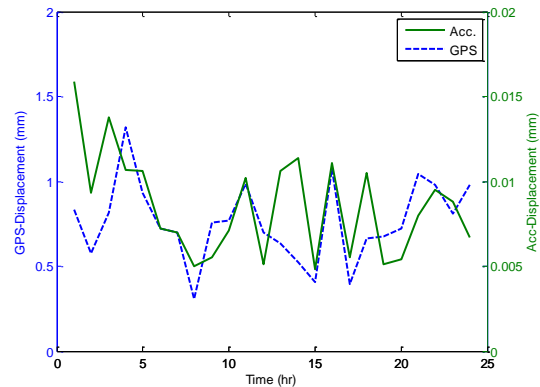
The damage effect increased the correlation between the GPS and accelerometer maximum dynamic displacement in both directions. Fig. 4-(c) shows high correlation (0.87) between the maximum dynamic displacement of both GPS and accelerometer X-direction, while the correlation is lower (0.66) in Y-direction as shown in Fig. 4-(d). It also can be noticed due to the damage occurrence that the maximum dynamic displacements of GPS are increased by 10 to 15 times; thus; the maximum dynamic displacements of the accelerometer observations are slightly increased. Furthermore, It can be seen from Fig. 4 that the dynamic displacement range (min. ~ max.), mean and standard deviation (SD) of maximum dynamic components in X-direction of the accelerometer observations is (0.06~0.68 mm), 0.34 mm and 0.18mm, respectively; while it is (0.44~1.76 mm), 0.98 mm and 0.34 mm, respectively, for the GPS observations, before the damage occurrence. In addition, after the damage and cracks

occurrence, the dynamic displacement range, mean and SD turns into (0.03~1.36 mm), 0.75 mm and 0.42mm, respectively, for the accelerometer observations, and (3.15~25.0 mm), 13.97 mm and 5.68 mm, respectively, for the GPS observations. Similarly, in Y-direction, the dynamic displacement range, mean and SD of the accelerometer observations changes from (0.004~0.015 mm), 8.5e-3 mm, 3e-3 mm to (0.002~0.032 mm), 18.7e-3 mm, 9.1e-3 mm, before and after the damage occurrence, respectively. While, the displacement range, mean and SD turns from (0.31~1.32 mm), 0.76 mm, 0.23 mm to (1.50~16.16 mm), 10.1 mm, 3.53 mm for the GPS observations due to the damage occurrence. Furthermore, F-test statistical analysis of dynamic displacement in the two directions of the movements with a 5 % level of significant based on a reference point was determined before the bridge loading (Kaloop and Li (2009)), show that the tower deformations are insignificant before damage occurred; while the deformation of the tower is high significant after the damage and cracks investigation, especially for the GPS monitoring system. It means that the statistical analysis of dynamic behavior can be used to detect the damage of bridge.

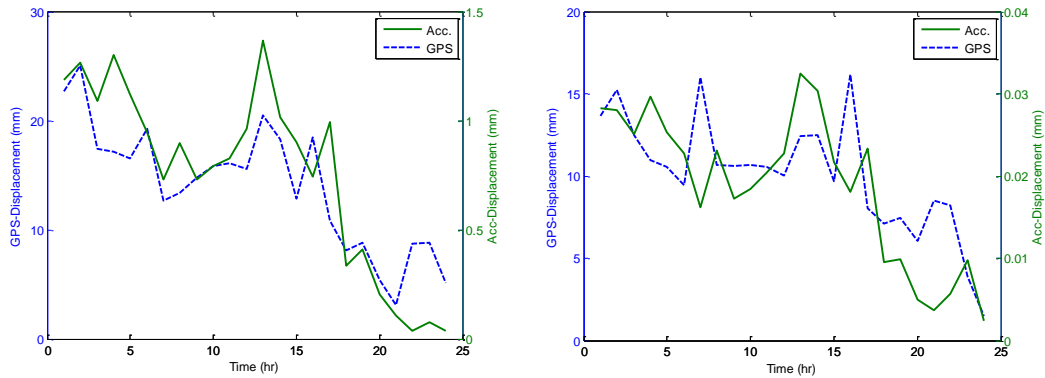
In addition, it can be noticed from Fig. 4-(c)&(d) that dynamic displacement for both GPS and accelerometer has fallen dramatically after the observation hour 18:00, where after that hour, the traffic and vehicle passage was prevented to observe the bridge tower displacement due to this prevention (Li et al. 2014), as shown in Fig. 2-(b). These results indicate that the effective load on the bridge deck and tower dynamic displacements is the vehicle-moving load. Finally, it can be concluded that using the bridge tower integrated system of GPS/accelerometer observations can be useful to detect the bridge cracks and damage effects, particularly in the bridge cables direction in time domain analysis.



(a) Before damage: X-direction



(b) Before damage: Y-direction



(c) After Damage: X-direction (d) After Damage: Y-direction
 Fig. 4. Maximum Dynamic Displacement Component of GPS and Accelerometer Observations of the Bridge Tower in Both Horizontal Directions

3.3. Comparative Fundamental Frequencies of GPS and Accelerometer Measurements

Table 1 illustrates the fundamental (first mode, which commonly used in the damage evaluations (Doebeling et al. 1996)) frequencies of the measured acceleration of the accelerometer sensor and the differentiated acceleration from the GPS displacement observations in the two horizontal directions for one day measurements. Table 1 illustrates that the fundamental frequencies range in X-direction of the measured acceleration of the accelerometer observations is (0.32-0.37) Hz and; while it is (0.21-0.37) Hz for the GPS calculated acceleration, before the damage occurrence. In addition, after the damage and cracks occurrence, the fundamental frequencies range turns into (0.25-0.27) Hz for the accelerometer observations, and (0.23-0.35) Hz for the GPS calculated acceleration observations. This variation in the frequency calculations occur because the accuracy of accelerometer for estimating dynamic behavior is high. Also, it can be noticed From Table 1 that the fundamental frequencies range of the accelerometer observations changes in Y-direction from (0.28-0.35) Hz to (0.25-0.28) Hz before the damage occurrence. While, the fundamental frequencies range turns from (0.23-0.39) Hz into (0.21-0.35) Hz for the GPS calculated acceleration after the damage occurrence. In addition, it can be noticed from Table 1 that the frequency range from the GPS observations is higher than that calculated from acceleration observations. In addition, it can be shown that the GPS fundamental frequency after traffic prevention (after hr 18:00) give non-conflicting results, while the accelerometer frequency range is approximately constant before and after the traffic prevention condition. However, the accelerometer is more sensitive in the damage detection in both horizontal direction of the bridge tower the frequency domain analysis. Furthermore, relative changes of frequencies ($RC = \frac{\text{absolute (frequency before damage - frequency after damage)}}{\text{frequency before damage}} \times 100$) are presented in Table 1. From the RC calculations values, the relative change of the fundamental frequency of GPS measurements in-between the healthy and damage cases are 0~31.6 and 0~35% in X- and Y- directions, respectively. Also, the range of the relative change of the accelerometer measurements in X and Y directions are 12.67~29.07 % and 4.47~27.01 %, respectively.

The previous results indicate that the fundamental frequency calculations of both the accelerometer and GPS observations gave close values to the fundamental frequency of the

bridge FEM in both X- and Y-direction before the damage occurrence on January 17th. In addition, due to the damage effect, the mean of the fundamental frequencies' changes of the accelerometer in between the two monitoring cases of the acceleration observations of the bridge tower decreased by 21 % and 17 % in the X- and Y-direction, respectively, and these values refer that the damage of bridge is occurred (Doebling *et al.*, 1996). Furthermore, the damage has slightly changed the fundamental frequencies of the calculated GPS acceleration measurements in both horizontal directions. These results imply that both the GPS and accelerometer can be used to detect the damage effect on the bridge tower separately; but the accelerometer observations are shown more effective in investigating the damage effect in the frequency domain analysis.

Table 1. Fundamental Frequencies and Relative Changes of the GPS and Accelerometer Acceleration Observations in X- And Y-Direction Before and After the Damage Occurrence

Time (h)	X-direction				Y-direction			
	GPS (Jan-Jul) (Hz)	RC(%)	Acc (Jan-Jul) (Hz)	RC(%)	GPS (Jan-Jul) (Hz)	RC(%)	Acc (Jan-Jul) (Hz)	RC(%)
1	0.27-0.23	14.26	0.33-0.26	21.12	0.31-0.21	31.26	0.33-0.26	21.12
2	0.25-0.25	0.00	0.35-0.26	23.28	0.27-0.25	7.13	0.33-0.26	20.39
3	0.33-0.25	23.52	0.32-0.27	16.06	0.33-0.25	23.52	0.35-0.27	22.25
4	0.33-0.23	29.40	0.33-0.26	19.37	0.31-0.25	18.75	0.33-0.27	17.32
5	0.29-0.25	13.34	0.34-0.27	20.62	0.37-0.25	31.58	0.34-0.27	21.09
6	0.29-0.25	13.34	0.33-0.26	19.14	0.31-0.25	18.75	0.30-0.26	13.16
7	0.27-0.25	7.13	0.33-0.26	19.07	0.23-0.25	8.32	0.31-0.26	15.65
8	0.27-0.25	7.13	0.36-0.26	27.29	0.33-0.25	23.52	0.33-0.26	20.61
9	0.33-0.25	23.52	0.32-0.26	17.04	0.29-0.25	13.34	0.32-0.27	16.01
10	0.27-0.25	7.13	0.34-0.26	21.65	0.29-0.25	13.34	0.32-0.26	17.34
11	0.25-0.27	7.68	0.32-0.26	17.62	0.25-0.27	7.68	0.30-0.26	13.90
12	0.27-0.25	7.13	0.34-0.26	22.68	0.29-0.25	13.34	0.35-0.26	24.22
13	0.21-0.27	27.28	0.33-0.26	21.08	0.23-0.25	8.11	0.36-0.26	27.01
14	0.31-0.29	6.24	0.32-0.26	17.40	0.33-0.25	23.67	0.33-0.26	20.42
15	0.37-0.25	31.58	0.37-0.26	29.07	0.39-0.25	35.00	0.30-0.26	12.93
16	0.35-0.25	27.79	0.33-0.26	21.47	0.37-0.25	31.58	0.31-0.26	16.87
17	0.21-0.25	18.20	0.35-0.26	26.24	0.33-0.25	23.52	0.30-0.26	13.04
18	0.33-0.27	17.65	0.33-0.25	21.70	0.37-0.25	31.72	0.33-0.25	23.36
19	0.23-0.25	8.32	0.35-0.26	24.25	0.29-0.23	20.00	0.29-0.27	6.82
20	0.25-0.33	30.76	0.35-0.26	24.00	0.23-0.27	16.64	0.30-0.26	14.94
21	0.23-0.27	16.64	0.33-0.26	21.68	0.31-0.25	18.91	0.34-0.26	22.66
22	0.29-0.29	0.00	0.33-0.26	20.11	0.35-0.35	0.00	0.34-0.27	19.41
23	0.33-0.35	5.90	0.36-0.27	26.55	0.29-0.29	0.00	0.30-0.26	12.80
24	0.31-0.27	12.51	0.30-0.26	12.67	0.37-0.25	31.72	0.30-0.29	4.47

4. CONCLUSIONS

Damage Assessment of Long-span Bridges using GPS/Accelerometer Observations under Dynamic Effects (10275)
 Mosbeh Kaloop (Republic of Korea), Mohamed Sayed (Canada) and Jong Hu (Republic of Korea)

FIG Working Week 2020
 Smart surveyors for land and water management
 Amsterdam, the Netherlands, 10–14 May 2020

The present study reports the assessment of the movement and damage effects of the cable-stayed Yonghe Bridge using the integrated monitoring system of GPS/accelerometer observations of the southern tower. The tower movement analysis in both horizontal directions is discussed in both time and frequency domains under the ambient environmental loads (wind and temperature) and vehicle loads in two monitoring cases: before and after the damage occurrence. The conclusions can be summarized as follows:

The short-period displacement component of the GPS is highly correlated with the dynamic displacements in the bridge cable X-direction due to the vibration in this direction. In contrast, less correlation is found in Y-direction due to the lack of the vibration and due to the high GPS signal noises in this direction. The damage and cracks increased the correlation between the maximum dynamic displacement of both GPS and accelerometer in both directions. In addition, the movement components are shown significantly with damage case. Although the bridge damage was located mainly in the bridge deck, however, the bridge tower suffers more displacements and vibrations after the damage occurrence due to the cables and the moving vehicle traffic. Load changes and damage effects throughout the monitoring time affect the bridge tower movements and cause 17 ~ 21 % changes in the fundamental frequency of the observation through the selection days. The integrated system of GPS/accelerometer observations is useful to detect the cracks and damage effects, particularly in the bridge cables direction.

The results reveal that GPS and accelerometer observations can be used separately to investigate and assess the tower movements and to evaluate the damage effects in time domain; while the accelerometer observations are more sensitive to the dynamic displacements and vibrations in both time and frequency domain. Nevertheless, the integrated system of the GPS/accelerometer observations and presented analysis methods are sufficiently effective for the movement assessment and damage effect detection in both horizontal directions of the bridge tower in time domain, whereas the accelerometer observations are more significant in frequency domain.

ACKNOWLEDGMENT

This work was supported by Basic Science Research Program through the National Research Foundation of Korea (NRF) funded by the Ministry of Science, ICT & Future Planning (2019R1I1A1A01062202).

REFERENCES

- Chan, W. S., Y. L. Xu, X. L. Ding, and W. J. Dai. 2006. "An Integrated GPS-Accelerometer Data Processing Technique for Structural Deformation Monitoring." *Journal of Geodesy* 80 (12): 705–19. <https://doi.org/10.1007/s00190-006-0092-2>.
- Chang, Peter C., Alison Flatau, and S. C. Liu. 2003. "Review Paper: Health Monitoring of Civil Infrastructure." *Structural Health Monitoring: An International Journal* 2 (3): 257–67. <https://doi.org/10.1177/1475921703036169>.
- Doebbling, Scott W Sw, Charles R Cr Farrar, Michael B Mb Prime, and Daniel W Dw Shevitz. 1996. "Damage Identification and Health Monitoring of Structural and Mechanical Systems from Changes in Their Vibration Characteristics: A Literature Review." *Los Alamos National Laboratory, University of California, USA*.

<https://doi.org/10.2172/249299>.

- Hwang, Jinsang, Hongsik Yun, Sun-Kyu Park, Dongha Lee, and Sungnam Hong. 2012. "Optimal Methods of RTK-GPS/Accelerometer Integration to Monitor the Displacement of Structures." *Sensors* 12 (1): 1014–34. <https://doi.org/10.3390/s120101014>.
- Im, Seok Been, Stefan Hurlbaeus, and Young Jong Kang. 2013. "Summary Review of GPS Technology for Structural Health Monitoring." *Journal of Structural Engineering* 139 (10): 1653–64. [https://doi.org/10.1061/\(ASCE\)ST.1943-541X.0000475](https://doi.org/10.1061/(ASCE)ST.1943-541X.0000475).
- Kaloop, M., and Li, H. 2009. "Monitoring of bridge deformation using GPS technique", *KSCCE Journal of Civil Engineering*, 13(6):423-431.
- Kaloop, Mosbeh, Emad Elbeltagi, Jong Hu, and Ahmed Elrefai. 2017. "Recent Advances of Structures Monitoring and Evaluation Using GPS-Time Series Monitoring Systems: A Review." *ISPRS International Journal of Geo-Information* 6 (12): 382. <https://doi.org/10.3390/ijgi6120382>.
- Kaloop, Mosbeh R., and Hui Li. 2014. "Multi Input-Single Output Models Identification of Tower Bridge Movements Using GPS Monitoring System." *Measurement: Journal of the International Measurement Confederation* 47 (1): 531–39. <https://doi.org/10.1016/j.measurement.2013.09.046>.
- Kaloop, Mosbeh R, and Jong Wan Hu. 2015. "Stayed-Cable Bridge Damage Detection and Localization Based on Accelerometer Health Monitoring Measurements." *Shock and Vibration* 2015 (Article ID 102680): 11 pages, doi: <http://dx.doi.org/10.1155/2015/1026>.
- Li, Shunlong, Hui Li, Yang Liu, Chengming Lan, Wensong Zhou, and Jinping Ou. 2014. "SMC Structural Health Monitoring Benchmark Problem Using Monitored Data from an Actual Cable-Stayed Bridge." *Structural Control and Health Monitoring* 21 (2): 156–72. <https://doi.org/10.1002/stc.1559>.
- Li, Xiaojing, Linlin Ge, Eliathamby Ambikairajah, Chris Rizos, Yukio Tamura, and Akihito Yoshida. 2006. "Full-Scale Structural Monitoring Using an Integrated GPS and Accelerometer System." *GPS Solutions*. <https://doi.org/10.1007/s10291-006-0023-y>.
- Meng, X., A. H. Dodson, and G. W. Roberts. 2007. "Detecting Bridge Dynamics with GPS and Triaxial Accelerometers." *Engineering Structures*. <https://doi.org/10.1016/j.engstruct.2007.03.012>.
- Moschas, Fanis, and Stathis Stiros. 2011. "Measurement of the Dynamic Displacements and of the Modal Frequencies of a Short-Span Pedestrian Bridge Using GPS and an Accelerometer." *Engineering Structures* 33 (1): 10–17. <https://doi.org/10.1016/j.engstruct.2010.09.013>.
- Moschas, Fanis, and Stathis Stiros. 2013. "Noise Characteristics of High-Frequency, Short-Duration GPS Records from Analysis of Identical, Collocated Instruments." *Measurement: Journal of the International Measurement Confederation* 46 (4): 1488–

Damage Assessment of Long-span Bridges using GPS/Accelerometer Observations under Dynamic Effects (10275)
Mosbeh Kaloop (Republic of Korea), Mohamed Sayed (Canada) and Jong Hu (Republic of Korea)

1506. <https://doi.org/10.1016/j.measurement.2012.12.015>.

- Roberts, Gethin Wyn, Xiaolin Meng, and Alan Henry Dodson. 2004. "Integrating a Global Positioning System and Accelerometers to Monitor the Deflection of Bridges." *Journal of Surveying Engineering* 130 (2): 65–72. [https://doi.org/10.1061/\(ASCE\)0733-9453\(2004\)130:2\(65\)](https://doi.org/10.1061/(ASCE)0733-9453(2004)130:2(65)).
- Yi, Ting Hua, Hong Nan Li, and Ming Gu. 2013. "Recent Research and Applications of GPS-Based Monitoring Technology for High-Rise Structures." *Structural Control and Health Monitoring*. <https://doi.org/10.1002/stc.1501>.
- Yi, Ting Hua, Hong Nan Li, and Xiao Yan Zhao. 2012. "Noise Smoothing for Structural Vibration Test Signals Using an Improved Wavelet Thresholding Technique." *Sensors (Switzerland)* 12 (8): 11205–20. <https://doi.org/10.3390/s120811205>.
- Zhang, J., J. Prader, K. A. Grimmelsman, F. Moon, A. E. Aktan, and A. Shama. 2013. "Experimental Vibration Analysis for Structural Identification of a Long-Span Suspension Bridge." *Journal of Engineering Mechanics*. [https://doi.org/10.1061/\(ASCE\)EM.1943-7889.0000416](https://doi.org/10.1061/(ASCE)EM.1943-7889.0000416).
- Zinno, Raffaele, Serena Artese, Gabriele Clausi, Floriana Magarò, Sebastiano Meduri, Angela Miceli, and Assunta Venneri. 2019. "Structural Health Monitoring (SHM)." In *Internet of Things*, 225–49. https://doi.org/10.1007/978-3-319-96550-5_10.

BIOGRAPHICAL NOTES and CONTACTS

Assoc. Prof. Mosbeh R.Kalooop

Department of Civil and Environmental Engineering, Incheon National University, Korea
Incheon Disaster Prevention Research Center, Incheon National University, Incheon, Korea
Email: mosbeh.kalooop@gmail.com, **Tel.:**+821082459298 (Corr. Author)

Dr. Mohamed A.Sayed

Department of Civil and Mineral Engineering, University of Toronto, Toronto, Canada

Assoc. Prof. Jong-Wan Hu

Department of Civil and Environmental Engineering, Incheon National University, Korea
Incheon Disaster Prevention Research Center, Incheon National University, Incheon, Korea